High-Sensitivity Temperature Sensor Based on a Coated Single-Mode Fiber Loop

Jun He, Changrui Liao, Kaiming Yang, Shen Liu, Guolu Yin, Bing Sun, Jiangtao Zhou, Jing Zhao, and Yiping Wang, *Senior Member, IEEE*

***Abstract*—We demonstrate a simple, robust, and highly sensitive temperature sensor based on the resonant excitation of whispering gallery modes in a coated single-mode fiber (SMF) loop that was created by means of bending a standard coated SMF into a loop with a radius of 5 mm. Clear interference fringes were observed in the transmission spectrum of the coated-SMF loop. The resonant wavelength exhibits a linear temperature response at the temperature range from −60° to 10 °C, and a quadratic temperature response at the temperature range from 10° to 140 °C. Moreover, the coated-SMF loop exhibits an ultrahigh sensitivity of up to −5.22 nm/°C at 120 °C, and the sensitivity (i.e., −4.01 nm/°C at 80 °C) is two orders of magnitude higher than that of an uncoated-SMF loop (i.e., 0.04 nm/°C at 80 °C). Hence, such a coated-SMF loop could be used to develop a temperature sensor with a large measurement range from −60° to 140 °C.**

***Index Terms*—Bending loss, modal interferometer, optical fiber sensors, whispering gallery mode (WGM).**

I. Introduction

In the past few decades, fiber-optic temperature sensors have been extensively studied due to the advantages of compact size, durability in harsh environment, immunity to electro- magnetic interference, and capability of remote interrogation. Numerous sensing schemes and devices have been developed for fiber-optic temperature sensors, such as fiber Bragg gratings (FBGs) [1], long-period fiber gratings (LPFGs) [2]–[4], in-fiber modal interferometers [5]–[7], and liquid-filled photonic crystal fibers (PCFs) [8]–[10]. Due to the limit of the thermal-optic coefficient of fused silica, the temperature-sensitivities of traditional FBGs, LPFGs, and interferometers are typically less than 0.1 nm/°C. Various techniques have been done to enhance the temperature-sensitivities. For example, Xue *et al.* sealed a microfiber taper in refractive index (RI) matching liquid, and achieved a temperature-sensitivity of −3.88 nm/°C [5]. Li *et al.* applied thermo-sensitive coatings on a modal interferometer, and achieved a sensitivity of 3.195 nm/°C [6]. Zhang *et al.* reported a higher sensitivity of 15 nm/°C by use of a similar technique [7]. Peiró *et al*. reported a liquid-filled PCF with an ultra-high sensitivity of 25 nm/°C [8]. Unfortunately, these techniques usually are too complicated to be realized.

A simple bent optical fiber loop could be used to solve the problem above. With the worldwide deployment of optical networks, the bending loss properties of optical fibers have been investigated thoroughly, including the bending loss oscillations in a coated single-mode fiber (SMF) [11]–[21]. Temperature sensors based on bent optical fibers have also been reported [22]–[26]. For example, researchers at Heriot-Watt University discovered the temperature-dependence of the bending loss in a SMF [22], [23]. Rajan *et al.* proposed a macro-bent SMF temperature sensor based on an absorptive coating layer and a ratio-metric power measurement scheme [25]. Nam and Yin reported a high-temperature sensor based on WGM excitation in a bent cladding-thinned uncoated SMF. Such a sensor exhibited a temperature-sensitivity of 0.212 nm/°C [26]. The relatively low temperature-sensitivities above result from the propagation of WGM in the insensitive cladding layers and/or the low-resolution intensity demodulation.

In this paper, we demonstrate a simple, robust, and highly-sensitive temperature sensor based on the resonant excitation of whispering gallery modes (WGMs) in a coated-SMF loop and wavelength demodulation. The sensor was created by means of bending a standard SMF with polymer coating layers into a loop with a radius of 5 mm. The coated-SMF loop exhibits an ultrahigh sensitivity of up to −5.22 nm/°C at 120 °C, and the sensitivity (i.e. −4.01 nm/°C at 80 °C) is two orders of magnitude higher than that of an uncoated-SMF loop (i.e. 0.04 nm/°C at 80 °C). The WGMs propagated in the thermal-sensitive coating layers and reflected at the coating-air boundary are responsible for the high temperature-sensitivity.

II. Resonant Excitation of WGMs in a Coated-SMF Loop

Fig. 1 illustrates the configuration and the principle of a coated-SMF loop temperature sensor. A normal SMF has four layers, i.e., fiber core, fiber cladding, inner coating, and outer coating. The fiber core and cladding are composed of fused silica, while the coating layers are composed of UV curable acrylate. As shown in Fig. 1, a modal interferometer could be developed to explain the resonant excitation of WGMs in a coated-SMF loop. While a coated SMF is bent into a loop with a small radius, the strain is generated along the fiber loop and

Manuscript received March 11, 2015; revised June 21, 2015 and July 11, 2015; accepted July 11, 2015. Date of publication July 13, 2015; date of current version August 17, 2015. This work was supported by the National Natural Science Foundation of China under Grants 61425007, 11174064, 61377090, and 61308027, the Natural Science Foundation of Guangdong under Grants 2014A030308007 and 2014A030312008, the Science and Technology Innovation Commission of Shenzhen/Nanshan under Grants KQCX20140512172532195, ZDSYS20140430164957664, and KC2014ZDZJ0008A, and the Pearl River Scholar Fellowships.

The authors are with the Key Laboratory of Optoelectronic Devices and Systems of Ministry of Education and Guangdong Province, College of Optoelectronic Engineering, Shenzhen University, Shenzhen 518060, China (e-mail: hejun07@szu.edu.cn; cliao@szu.edu.cn; yangkaiming@email.szu.edu.cn; liushen.szu@gmail.com; guoluyin@gmail.com; pcf13@szu.edu.cn; 2121190102@email.szu.edu.cn; Zhaojing090824@163.com; ypwang@szu.edu.cn).

Color versions of one or more of the figures in this paper are available online at http://ieeexplore.ieee.org.

Digital Object Identifier 10.1109/JLT.2015.2456153

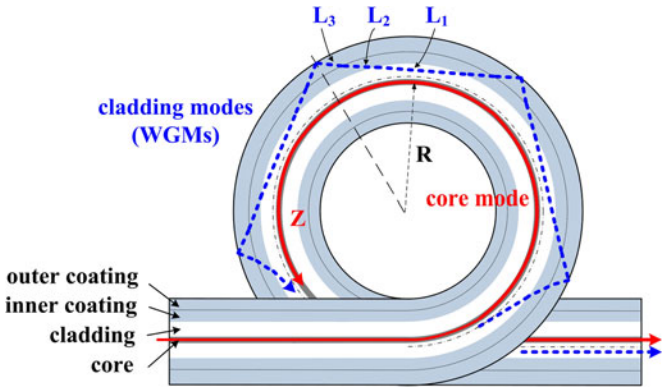

Fig. 1. Schematic diagram of the coated-SMF loop temperature senor and the resonant excitation of whispering gallery modes (WGMs).

produces anisotropic and asymmetric changes of the dielectric constant due to the photo-elastic effect [16]–[21]. In addition, the geometrical effect associated with the curvature of fiber can also change the effective refractive index (RI) profile [19]–[21]. As a result, the modal index of the higher-order cladding modes increases strongly, whereas the modal index of the fundamental core mode increases slightly. When the modal index is matched, a resonant coupling between the core mode and the cladding modes is produced, and efficient power transfer from the core mode to the cladding modes is enabled. Some cladding modes are absorbed by the coating layers or lost in the form of leaky modes, thus giving rise to an intrinsic bending loss of the core mode, especially at longer wavelength.

Furthermore, a number of cladding modes propagate in the cladding and coating layers in the form of whispering gallery modes (WGMs) [12]–[21]. Due to the much larger RI contrast, the reflection at the coating-air boundary is much larger than that at the cladding-coating boundary, and plays a decisive role in the formation of WGMs. And eventually, the WGMs in the cladding and coating layers interfere with the fundamental core mode at the output of the loop when the curvature disappears. The resonant coupling takes place at the wavelength where a phase matching condition is satisfied, and hence gives rise to an attenuation dip in the transmission spectrum of the core mode. In order to implement a coated-SMF loop temperature sensor, we can take advantage of the temperature dependence of the modal index of WGMs, which leads to a wavelength shift in the transmission dip as a function of the ambient temperature.

The phase difference $\Delta\phi_k$ between the kth WGM and the core mode can be expressed as [27]

$$\Delta\phi_k = (\beta_{\mathrm{WGM},k} - \beta_{co})\, Z = \frac{2\pi}{\lambda}\left(l_{\mathrm{WGM},k} - n_0 Z\right), \qquad (1)$$

where $\beta_{\mathrm{WGM},k}$ and β_{co} are the propagation constants of the kth WGM and the core mode, respectively; Z is the arc length of the fiber loop; λ is the wavelength; n_0 is the effective RI of the fiber core mode; $l_{\mathrm{WGM},k}$ is the optical path length of the WGM and can be given by

$$l_{\mathrm{WGM},k} = 2\left(n_{cl}L_1 + n_{b1}L_2 + n_{b2}L_3\right), \qquad (2)$$

where L_1, L_2, and L_3 are the WGM trace lengths in the cladding layer, inner coating layer, and outer coating layer, respectively; n_{cl}, n_{b1}, and n_{b2} are the effective RIs of the three layers above, respectively. It should be stated that a ray model is developed in Eq. (2) for simplicity, whereas the previous descriptions in this paper is focused on a modal approach. Nevertheless, Eq. (2) is enough for qualitatively analyzing the experimental results.

The mth resonant wavelength λ_m in the transmission spectrum should satisfy the phase condition below [12], [14], [15], [27]

$$\Delta\phi_k = \frac{2\pi}{\lambda_m}\left(l_{\mathrm{WGM},k} - n_0 Z\right) = (2m+1)\,\pi. \qquad (3)$$

In order to derive the temperature sensitivities of the resonant wavelength in the transmission spectrum, Eq. (2) is substituted into Eq. (3), and then the differentiation is done. So the temperature-sensitivity of a coated-SMF loop should be

$$m\frac{d\lambda_{m,c}}{dT} = \underbrace{2L_2\left(\mu_{b1} + n_{b1}\xi_{b1}\right) + 2L_3\left(\mu_{b2} + n_{b2}\xi_{b2}\right)}_{\text{Coating layer}} + \underbrace{2L_1\left(\mu_{cl} + n_{cl}\xi_{cl}\right)}_{\text{Cladding layer}} - \underbrace{Z\left(\mu_0 + n_0\xi_0\right)}_{\text{Fiber core}}, \qquad (4)$$

where dT is the temperature change; n_0, n_{cl}, n_{b1}, and n_{b2} are the RIs, $\mu_0, \mu_{cl}, \mu_{b1}$, and μ_{b2} are the thermo-optic coefficients (TOCs); $\xi_0, \xi_{cl}, \xi_{b1}$, and ξ_{b2} are the thermal expansion coefficients (TECs). The subscripts 0, cl, b1, and b2 refer to the fiber core, fiber cladding, inner coating, and outer coating, respectively. Table I shows the typical parameters of a standard Corning SMF-28 fiber.

TABLE I
TYPICAL PARAMETERS OF A STANDARD CORNING SMF-28 FIBER[a] [18], [24], [28]

Parameters (units)		Core	Cladding	Inner coating	Outer coating
material		Ge-doped silica	silica	UV curable acrylate	
radius	r (μm)	4.15	62.5	95	125
RI	n	1.4504	1.4447	1.4786	1.5294
TEC	ξ (K^{-1})	5.5×10^{-7}	5.5×10^{-7}	8.0×10^{-5}	$<1.0\times10^{-5}$
TOC	μ (K^{-1})	7.97×10^{-6}	7.80×10^{-6}	-2.90×10^{-3}	

[a] Measured at 25 °C and 1550 nm.

For a coated-SMF loop, the first two items in the right side of Eq. (4) depend on the coating material, the third item depends on the fiber cladding material, and the last item depends on the fiber core material. For an uncoated-SMF loop, the first two items do not exist, and the TEC of fused silica is much smaller than the TOC [24]. So the temperature-sensitivity of an uncoated-SMF loop can be simplified as

$$m\frac{d\lambda_{m,u}}{dT} \approx (2L_1 - Z)\,\mu_{cl}. \qquad (5)$$

Since the UV curable acrylate in the coating layers has a much larger TOC than the fused silica in the fiber core and the fiber cladding layer (i.e., -2.90×10^{-3}/°C for UV curable acrylate [24], 7.80×10^{-6}/°C for silica, and 7.97×10^{-6}/°C for Ge-doped silica [28]), a much higher temperature-sensitivity can be expected in a coated-SMF loop.

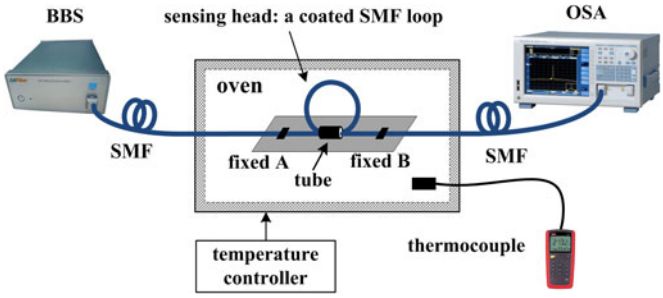

Fig. 2. Experimental setup for testing the coated-SMF loop temperature senor (BBS: broadband light source, OSA: optical spectrum analyzer, SMF: single-mode fiber).

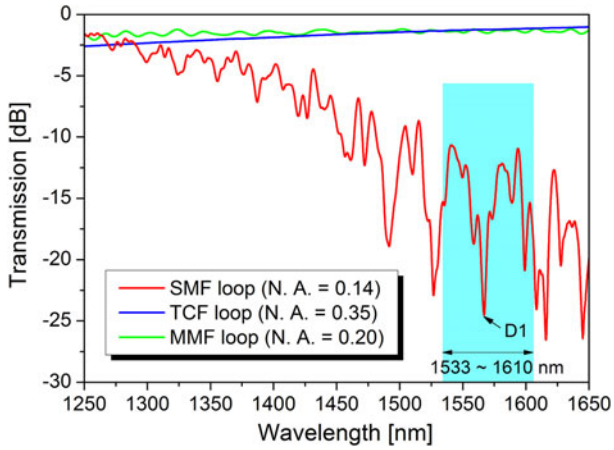

Fig. 3. Transmission spectra of the coated-SMF, -TCF, and -MMF loops (R = 5 mm, T = 25 °C) measured by use of a broadband light source and an optical spectrum analyzer. (Note that the transmission spectrum of the coated-SMF loop in the wavelength range from 1533 to 1610 nm (light-blue region) was further investigated by use of a tunable laser source, a polarization synthesizer, and a power meter, as shown in Fig. 4.).

III. Experimental Results and Discussions

A. Construction of a Coated-SMF Loop and Measurement of the Transmission Spectrum

As shown in Fig. 2, a fiber loop was constructed by means of bending a coated optical fiber through a metal tube with an inner diameter of 1 mm and a length of 3 mm. And then the fiber loop was fixed onto a steel plate by employing UV curable adhesive on the two leading fibers and on the tube. With the protection of the coating layers, the coated fiber loop was robust and could hardly be broken. The steel plate with the fixed loop was placed into an oven in which the temperature can be controlled. A differential thermocouple (UNI-T UT320) was used to measure the temperature with an accuracy of 0.1 °C. A broadband light source (BBS, Fiber-Lake FL-ASE-EB) and an optical spectrum analyzer (OSA, YOKOGAWA AQ6370C) were used to measure the transmission spectra (i.e. bending loss spectra) of the fiber loop. The BBS was based on amplified spontaneous emission (ASE) of four-channel semiconductor optical amplifiers (SOAs), and had a wavelength range from 1250 to 1650 nm (i.e. a bandwidth of 400 nm), an output power of 10.79 dBm, a power stability of ± 0.02 dB, and a degree of polarization (DOP) of less than 5%. The OSA was scanned from 1250 to 1650 nm with a wavelength resolution of 0.5 nm and a 'HIGH1' sensitivity mode.

In our experiments, three types of optical fibers, i.e., a standard SMF (Corning SMF-28, N. A. $= 0.14$), a thin-core single-mode fiber (TCF, Nufern UHNA-3, N. A. $= 0.35$), and a graded-index multimode fiber (MMF, YOFC, N. A. $= 0.20$), with different numerical apertures (N. A.s) were used to construct the coated fiber loop sensors. The three types of fibers were bent into three different loops, i.e., the SMF loop, the TCF loop, and the MMF loop, with the same radius of 5 mm. As shown in Fig. 3, clear interference fringes and a larger bending loss were observed in the transmission spectrum of the coated-SMF loop. In contrast, no interference fringes were observed in the transmission spectra, with a smaller bending loss, of the coated-TCF and -MMF loops.

Since the TCF has a much larger N. A. than a standard SMF, phase matching between the WGMs and the core mode should take place in the coated-TCF loop with a much smaller radius, and efficient power transfer will not happen in the coated-TCF loop with the same radius of 5 mm as that of the coated-SMF loop. So the coated-TCF loop, as shown in Fig. 3, has no clear interference fringes in the transmission spectrum, together with a much smaller bending loss. In the case of the coated-MMF loop, there are hundreds of modes in the fiber core, and multiple interferences should take place between the WGMs and core modes. Due to the averaging effect, no inference fringes could be seen in a coated-MMF loop. Therefore, only the standard SMF was employed to demonstrate coated fiber loop sensors in the following experiments.

B. Polarization Dependence of the Coated-SMF Loop

The polarization dependence of the coated-SMF loop was investigated by use of a linear-polarized tunable laser source (Agilent, model 81940A), a polarization synthesizer (Agilent, model N7786B), and an optical power meter (Agilent, model N7744A). The wavelength of the tunable laser was scanned from 1533 to 1610 nm with a resolution of 0.015 nm. At each test wavelength, a set of polarization states was generated sequentially by the polarization synthesizer, and sent into the coated-SMF loop. After the output power of the coated-SMF loop was detected by the optical power meter, the transmission spectra of two orthogonal polarization modes (TE and TM), the average insertion loss (IL) spectrum, and the polarization dependent loss (PDL) were measured via Mueller matrixes. The same transmission dip D1, as shown in Figs. 3 and 4, was measured by use of the same coated-SMF loop but different methods and equipments.

As shown in Fig. 4, the transmission spectra of the TE and TM modes have a much larger fringe contrast of 24.76 and 31.36 dB, respectively, than the fringe contrast of 14.53 dB in the average IL spectrum. Moreover, the transmission spectra of the TE and TM modes are quite similar, unless a spectral shift of 2.72 nm is observed. The maximum PDL of the coated-SMF loop is up to 32.42 dB. The high birefringence in the coated-SMF loop may result from the large anisotropic stress induced by fiber macro-bending.

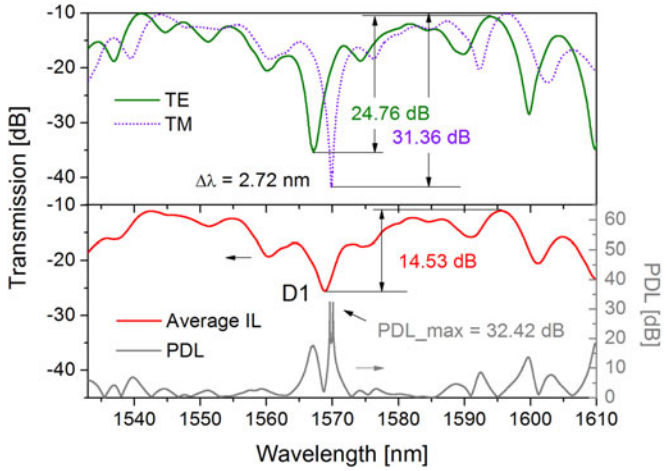

Fig. 4. Polarization dependence of the coated-SMF loop (Corning SMF-28, R = 5 mm, T = 25 °C) measured by use of a tunable laser source, a polarization synthesizer, and a power meter. Upper panel: transmission spectra of two orthogonal polarization modes (TE and TM); Lower panel: average insertion loss spectrum (IL, left axis) and polarization dependent loss (PDL, right axis).

Furthermore, it should be noted that due to the limit of the wavelength range of the tunable laser source, the transmission spectra in the following experiments were all measured by use of the BBS and OSA, instead of the tunable laser, polarization synthesizer, and optical power meter.

C. Temperature Response of the Coated-SMF Loops

Three types of SMFs available in our lab, i.e., Corning SMF-28, YOFC SMF, and Draka SMF, were employed to investigate the temperature response of the coated-SMF loops with the same radius of 5 mm. The three types of SMFs were supplied by different manufacturers, and had similar optical specifications (such as mode-field diameters, N. A.s, and cutoff wavelengths) but different parameters in the coating layers. As shown in Fig. 5(b), the Corning SMF-28 and the YOFC SMF have similar coatings with transparent colors, whereas the Draka SMF has a different coating with a green color.

While the three coated-SMF loops (i.e., Corning-SMF-28 loop, YOFC-SMF loop, and Draka-SMF loop) were placed in the oven, the temperature was gradually increased from −60 to 150 °C, and the transmission spectra were measured with a step of 10 °C. The transmission spectra of the three coated-SMF loops at several typical temperatures of −60, 20, 80, 140 and 150 °C were illustrated in Fig. 5(a). At temperatures lower than 140 °C, all of the three coated-SMF loops have clear interference fringes. At higher temperatures, the fringes of the Corning-SMF-28 loop and the YOFC-SMF loop disappear gradually, but clear fringes are remained in the Draka-SMF loop, even at 150 °C. Higher temperatures have not been applied due to the limit of the oven used in our experiments.

The temperature-sensitivities are derived from the slope of the temperature response. All of the three coated-SMF loops exhibit high temperature-sensitivities. As shown in Fig. 5(d), the Corning-SMF-28, YOFC-SMF, and Draka-SMF loops have a high temperature-sensitivity of −1.39, −1.29,

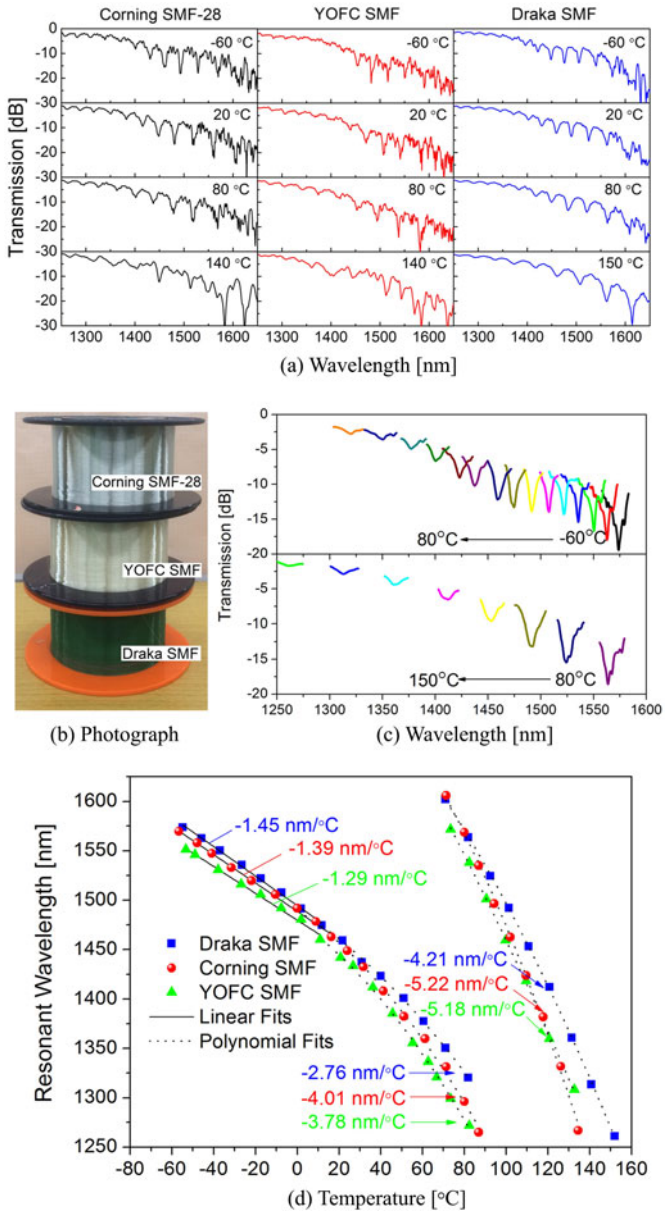

Fig. 5. (a) The transmission spectra of the three types of coated-SMF loops (Corning SMF-28, YOFC SMF, Draka SMF, R = 5 mm) at typical temperatures of −60, 20, 80, 140 and 150 °C; (b) The photograph of the three types of SMFs; (c) Resonant wavelength evolution of the Draka-SMF loop with a step of 10 °C (upper: evolution of the transmission dip around 1570 nm at the initial temperature of −60 °C, lower: evolution of the transmission dip around 1570 nm at the initial temperature of 80 °C); (d) The temperature response of the three types of coated-SMF loop sensors.

and −1.45 nm/°C at the temperature range from −60 to 10 °C, a higher temperature-sensitivity of −4.01, −3.78, and −2.76 nm/°C at 80 °C, and an ultrahigh temperature-sensitivity of −5.22, −5.18, and −4.21 nm/°C at 120 °C. Compared with the Corning-SMF-28 loop, the Draka-SMF loop has a better linearity but a slightly lower temperature-sensitivity.

In order to fast sweep the wavelength range of 400 nm, the wavelength resolution used in Fig. 5 was 0.5 nm. Hence, the temperature resolution of the coated-SMF loop was around 0.4 °C at low temperature and around 0.1 °C at high temperature.

The temperature resolution could further be improved by use of a high-resolution wavelength interrogator and a resonant-wavelength-seeking algorithm.

The experimental results shown in Fig. 5 can be quantitatively explained by use of Eq. (4). For a coated-SMF loop, the WGMs propagate in the coating layers and the cladding layer. As shown in Table I, the TOC of the UV curable acrylate μ_b is negative and the absolute value is large ($\mu_b = -2.9 \times 10^{-3}$/°C [24]). Hence, the coated-SMF loop has a high temperature-sensitivity with a negative value ('blue' shift). The nonlinear temperature response of the coated-SMF loop may probably result from the change in μ_b with rising temperature. μ_b is a constant at lower temperature, so that the coated-SMF loop exhibits a linear temperature response at the temperature range from -60 to 10 °C, as shown in Fig. 5(d). In contrast, an increasing μ_b at the temperatures higher than 10 °C leads to a quadratic response with an increasing sensitivity. The analysis agrees well with the measurement results reported in [29], in which the TOC is two-times larger at higher temperatures. Moreover, the differences between the temperature response of the Draka-SMF loop and that of the Corning-SMF-28 loop is due to the slightly different μ_b of the coating materials, especially at high temperatures.

D. Coated-SMF Loops With Different Bend Radius

The temperature response of the coated-SMF loops with different bend radius was investigated to improve the loop radius for temperature sensing applications. Due to the relatively high sensitivity, the Corning SMF-28 fiber was used in this experiment. As shown in Fig. 6(a), the intrinsic bending loss of the coated-SMF loop increase with the decrease of the loop radius, and the fringe contrast is larger at longer wavelengths. This phenomenon may result from an enhanced resonant excitation of WGMs in the coated-SMF loop with a smaller radius and at longer wavelengths. In case the power of WGM is equal to that of core mode, the destructive interference is optimum with the largest fringe contrast. With a bend radius of around 5 mm, a fringe contrast of more than 10 dB can be achieved at 1550 nm with an acceptable intrinsic bending loss. When the bend radius is larger than 6 mm, the fringe contrast is too small to be detected. When the radius is smaller than 4 mm, the interference fringes are in disorder, which may result from the higher-order WGMs interference. The free spectra range (FSR) of the interference fringes, defined as the difference between two adjacent resonant wavelengths, decreases with the bend radius reducing, which is in agreement with the previous reports [13]. As the radius is reduced, the number of WGMs that phase match the core mode increases in a given wavelength range, and the interference of WGMs and core mode generates a larger number of dips in the transmission spectrum.

As shown in Fig. 6(b), the coated-SMF loops with a radius of 7.08, 5.85, 4.91, and 3.74 mm exhibit a temperature-sensitivity of −3.86, −3.35, −2.65, and −2.14 nm/°C, respectively. In other words, a larger SMF loop has a higher temperature-sensitivity. It can be seen from Eq. (4) that in case of a coated-SMF loop with a larger radius, the temperature-sensitivity should increase with a longer length L_2 and L_3 in the coating layers. Considering the fringe contrast and the temperature-sensitivity, the optimum radius of a coated-SMF loop should be 5 mm.

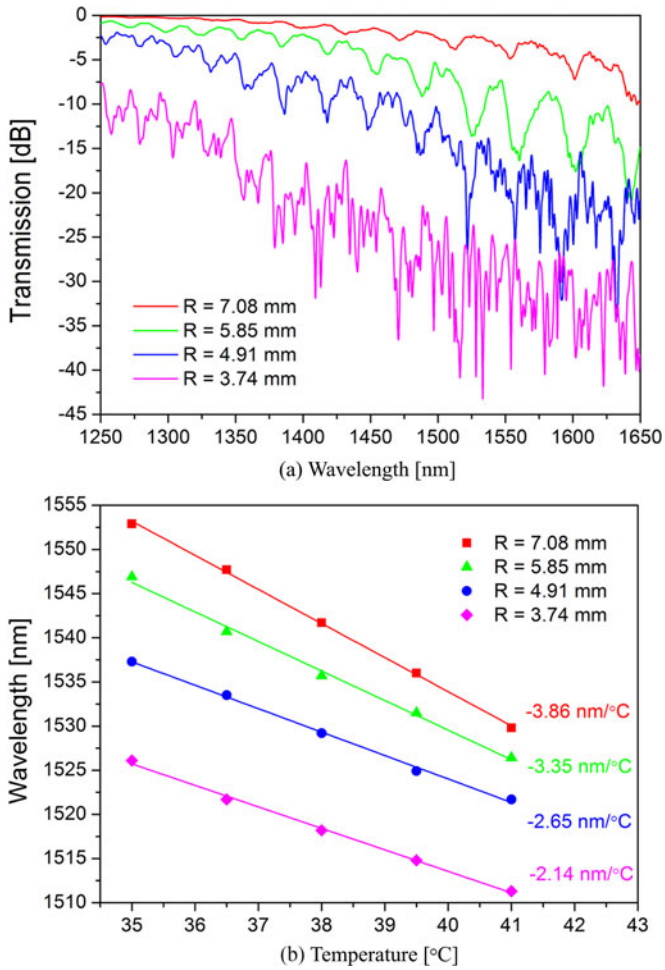

Fig. 6. (a) Transmission spectra of the coated-SMF loops with different bend radius (Corning SMF-28, T = 25 °C); (b) Temperature-sensitivities of the coated-SMF loops with different bend radius.

E. Temperature Response of the Uncoated-SMF Loop

The temperature response of an uncoated-SMF loop was investigated to compare with that of a coated-SMF loop. The coating layers of a standard Corning SMF-28 fiber were removed in advance. And then the uncoated fiber was bent into a loop with a radius of 5 mm by using the same method described above. Without the protection of coating layers, the uncoated-SMF loop was much more fragile than the coated- SMF loop. As shown in Fig. 7(a), clear interference fringes have been achieved in the transmission spectra of the uncoated- SMF loop. As shown in the inset of Fig. 7(a), the interference fringes shifted toward a longer wavelength (i.e. 'red' shift) with rising temperature. As shown in Fig. 7(b), the temperature- sensitivity of the uncoated-SMF loop is 0.04 nm/°C. It can be seen from Figs. 5 and 7 that the temperature response of the coated-Corning-SMF loop is completely different from that of an uncoated-Corning-SMF loop with the same bend radius. That is, the coated-Corning-SMF loop exhibits a 'blue' shift with an ultrahigh sensitivity of

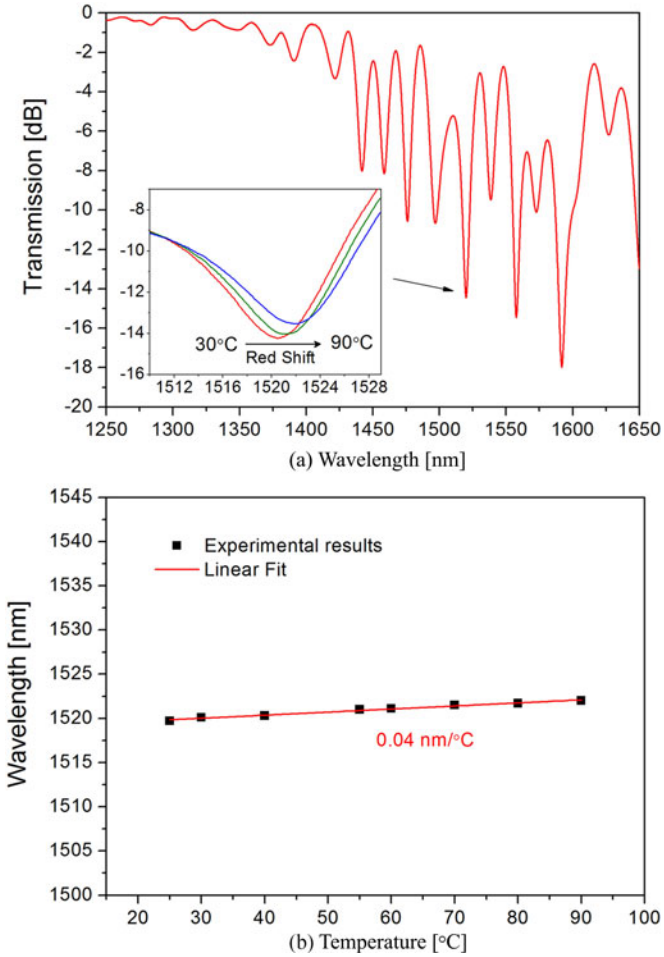

Fig. 7. (a) Transmission spectrum of the uncoated-SMF loop (Corning SMF-28, R = 5 mm), inset: interference fringes at different temperatures; (b) Temperature response of the uncoated-SMF loop.

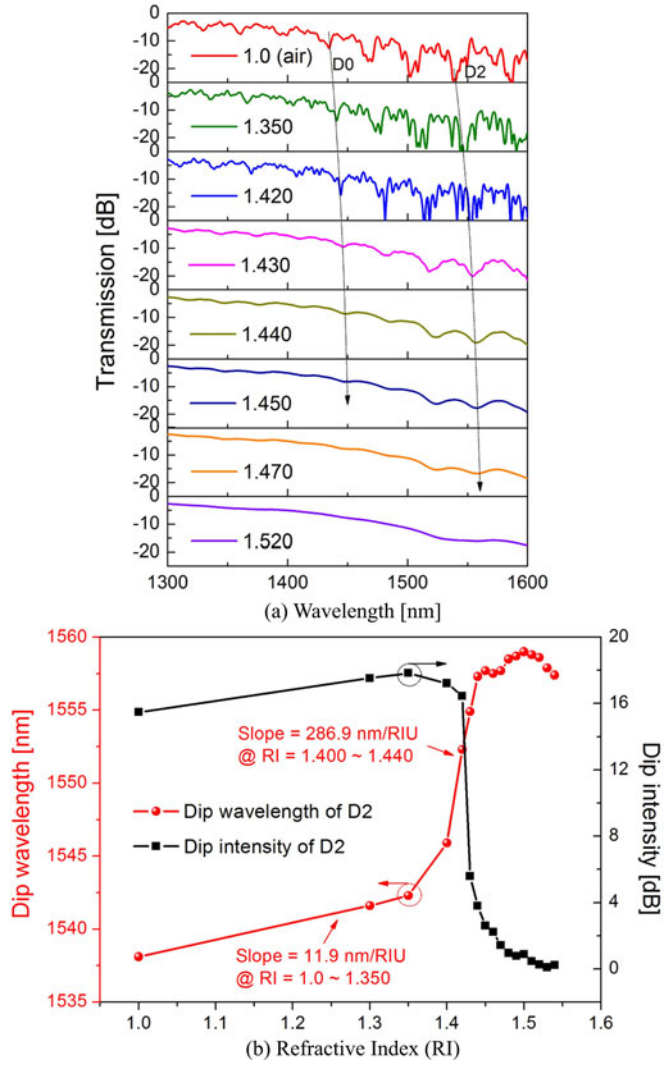

Fig. 8. (a) Transmission spectrum evolution of a coated-SMF loop immerged into different refractive index matching liquids (Corning SMF-28, R = 5 mm, T = 25 °C); (b) Measured dip wavelength and dip intensity of the transmission dip D2 as a function of the surrounding refractive index.

−4.01 nm/°C at 80 °C, whereas, an uncoated-Corning-SMF loop exhibits a 'red' shift with a much lower sensitivity of 0.04 nm/°C at the same temperature.

The differences between the experimental results in Figs. 5 and 7 can be quantitatively explained via the temperature-sensitivities, as given in Eq. (4) and (5), of the coated- and uncoated-SMF loops. For an uncoated-SMF loop, the WGMs propagate in the cladding layer. As shown in Table I, the TOC of the silica μ_{cl} is positive, and the trace length of the WGM ($2L_1$) is slightly longer than that of the core mode (Z). Hence, the temperature-sensitivity of an uncoated-SMF loop should be positive ('red' shift). For a coated-SMF loop, the WGMs propagate in the coating layers as well as in the cladding layer. As shown in Table I, the TOC of the UV curable acrylate μ_b is negative ($\mu_b = -2.9 \times 10^{-3}$/°C [24]), and the absolute value is two orders larger than that of the fused silica ($\mu_{cl} = 7.8 \times 10^{-6}$/°C [28]). Therefore, the temperature-sensitivity of a coated-SMF loop should be negative ('blue' shift), and will be much larger than that of an uncoated-SMF loop. The experimental results are in accordance with theoretical expectations.

F. Response of the Coated-SMF Loop to Surrounding RI

We also investigated the response of the coated-SMF loop to surrounding refractive index (RI) by means of immersing the loop into a series of refractive index matching liquids (Cargille Labs). A coated-Corning-SMF-28 loop with a radius of 5 mm was used. The ambient temperature and the strain within the loop were kept unchanged during the experiment.

As shown in Fig. 8, the RI response of the coated-SMF loop was investigated by use of the dip wavelength (i.e. resonant wavelength) and dip intensity (i.e. interference fringe contrast) of the transmission dip D2. In case the surrounding RI was increased from 1.0 to 1.420, the dip wavelength shifted toward a longer wavelength (i.e. 'red' shift), whereas the dip intensity hardly changed. In case the surrounding RI was increased from 1.420 to 1.440, the dip intensity was reduced drastically from 16.45 to 3.79 dB, and the dip wavelength further shifted toward a longer wavelength. In case the surrounding RI was

increased from 1.440 to 1.520, the dip intensity was further reduced from 3.79 to 0.09 dB, whereas the dip wavelength hardly changed. The interference fringes almost disappeared in case the RI was further increased to a higher value of 1.520, which is nearly equal to the effective RI of the outer coating layer. As shown in Fig. 8(b), the RI sensitivity of the coated-SMF loop is 11.9 nm/RIU in the RI range of $1.0 \sim 1.350$, and increases to a higher value of 286.9 nm/RIU in the RI range of $1.400 \sim 1.440$.

The reason for the RI sensitivity is that the WGMs in the coated-SMF loop propagate in the coating layers and are guided by the confinement of coating-air boundary. The modal index of WGMs increases with an increasing external RI [19], [27], and leads to a decrease in the coupling efficiency between WGMs and core mode, and eventually results in a decrease in the dip intensity. In addition, it can be seen from Eq. (1) that the phase difference between WGMs and core mode increases, and hence leads to a 'red' shift in the dip wavelength. In case the external RI is equal to the effective RI of the outer coating layer, there is no total internal reflection at the coating-air boundary, and thus no WGM can be guided any more. In other words, the WGMs do not exist, and only radiation modes can exist. Therefore, the interference fringes disappear in the transmission spectrum, and there remains only an intrinsic loss at longer wavelength.

Moreover, the cross sensitivity between temperature and surrounding RI could be avoided by appropriately packaging the coated-SMF loop temperature sensor. And in this way, the influence of environmental humidity and contaminations could be eliminated in the measurement of temperature.

In the future, such a coated-SMF loop could also be used to develop a promising chemical and bio-photonic sensor owing to its high sensitivity to changes in the surrounding mediums refractive index.

IV. Conclusion

A coated-SMF loop was demonstrated to develop a high- sensitivity temperature sensor based on the resonant excitation of WGMs. The sensor was constructed by means of bending a standard SMF into a fiber loop with a radius of 5 mm. Temperature-dependent interference fringes were observed in the transmission spectrum of the coated-SMF loop. An ultrahigh sensitivity of -5.22 nm/°C and a large measurement range from -60 °C to 140 °C were achieved. Moreover, the coated-SMF loop exhibits a much higher sensitivity than the uncoated-SMF loop. The proposed coated-SMF loop sensor provides a promising way for low-cost, high-performance temperature measurement.

References

[1] A. D. Kersey, M. A. Davis, H. J. Patrick, M. LeBlanc, K. P. Koo, C. G. Askins, M. A. Putnam, and E. J. Friebele, "Fiber grating sensors," *J. Lightw. Technol.*, vol. 15, no. 8, pp. 1442–1463, Aug. 1997.

[2] Y. P. Wang, "Review of long period fiber gratings written by CO_2 laser," *J. Appl. Phys.*, vol. 108, no. 8, p. 081101, Oct. 2010.

[3] G. L. Yin, Y. P. Wang, C. R. Liao, J. T. Zhou, X. Y. Zhong, G. J. Wang, B. Sun, and J. He, "Long period fiber gratings inscribed by periodically tapering a fiber," *IEEE Photon. Technol. Lett.*, vol. 26, no. 7, pp. 698–701, Apr. 2014.

[4] Y. P. Wang, J. P. Chen, and Y. J. Rao, "Torsion characteristics of long-period fiber gratings induced by high-frequency CO_2 laser pulses," *J. Opt. Soc. Amer. B.*, vol. 22, no. 6, pp. 1167–1172, Jun. 2005.

[5] Y. Xue, Y. S. Yu, R. Yang, C. Wang, C. Chen, J. C. Guo, X. Y. Zhang, C. C. Zhu, and H. B. Sun, "Ultrasensitive temperature sensor based on an isopropanol-sealed optical microfiber taper," *Opt. Lett.*, vol. 38, no. 8, pp. 1209–1211, Apr. 2013.

[6] E. B. Li and G. D. Peng, "Wavelength-encoded fiber-optic temperature sensor with ultra-high sensitivity," *Opt. Commun.*, vol. 281, no. 23, pp. 5768–5770, Dec. 2008.

[7] Y. J. Zhang, L. L. Xue, T. X. Wang, L. Yang, B. Zhu, and Q. J. Zhang, "High performance temperature sensing of single mode-multimode- single mode fiber with thermo-optic polymer as cladding of multimode fiber segment," *IEEE Sens. J.*, vol. 14, no. 4, pp. 1143–1147, Apr. 2014.

[8] S. T. Peiró, A. Díez, J. L. Cruz, and M. V. Andrés, "Sensor applications based on the cutoff properties of liquid-filled Ge-doped microstructured fibers," *IEEE Sens. J.*, vol. 10, no. 7, pp. 1174–1179, Jul. 2010.

[9] Y. P. Wang, X. L. Tan, W. Jin, D. Q. Ying, Y. L. Hoo, and S. J. Liu, "Temperature-controlled transformation in fiber types of fluid-filled photonic crystal fibers and applications," *Opt. Lett.*, vol. 35, no. 1, pp. 88–90, Jan. 2010.

[10] Y. Wang, M. W. Yang, D. N. Wang, and C. R. Liao, "Selectively infiltrated photonic crystal fiber with ultrahigh temperature sensitivity," *IEEE Photon. Technol. Lett.*, vol. 23, no. 20, pp. 1520–1522, Oct. 2011.

[11] Y. Murakami and H. Tsuchiya, "Bending losses of coated single-mode optical fibers," *IEEE J. Quantum Electron.*, vol. QE-14, no. 7, pp. 495–501, Jul. 1978.

[12] J. Harris and P. F. Castle, "Bend loss measurements on high numerical aperture single-mode fibers as a function of wavelength and bend radius," *J. Lightw. Technol.*, vol. LT-4, no. 1, pp. 34–40, Jan. 1986.

[13] G. L. Tangonan, H. P. Hsu, V. Jones, and J. Pikulski, "Bend loss measurements for small mode field diameter fibers," *Electron. Lett.*, vol. 25, no. 2, pp. 142–14, Jan. 1989.

[14] R. Morgan, J. S. Barton, P. G. Harper, and J. D. C. Jones, "Wavelength dependence of bending loss in monomode optical fibers: effect of the fiber buffer coating," *Opt. Lett.*, vol. 15, no. 17, pp. 947–949, Sep. 1990.

[15] R. D. Morgan, J. D. C. Jones, J. S. Barton, and P. G. Harper, "Determination of monomode fiber buffer properties," *J. Lightw. Technol.*, vol. 12, no. 8, pp. 1355–1359, Aug. 1994.

[16] L. Faustini and G. Martini, "Bend loss in single-mode fibers," *J. Lightw. Technol.*, vol. 15, no. 4, pp. 671–679, Apr. 1997.

[17] Q. Wang, G. Rajan, P. F. Wang, and G. Farrell, "Polarization dependence of bend loss for a standard singlemode fiber," *Opt. Exp.*, vol. 15, no. 8, pp. 4909–4920, Apr. 2007.

[18] P. F. Wang, Q. Wang, G. Farrell, G. Rajan, T. Freir, and J. Cassidy, "Investigation of macrobending losses of standard single mode fiber with small bend radii," *Microw. Opt. Technol. Lett.*, vol. 49, no. 9, pp. 2133–2138, Sep. 2007.

[19] M. Reyes, D. M. Hernández, A. M. Ríos, E. Silvestre, A. Díez, J. L. Cruz, and M. V. Andrés, "A refractive index sensor based on the resonant coupling to cladding modes in a fiber loop," *Sensors*, vol. 13, no. 9, pp. 11260–11270, Sep. 2013.

[20] R. T. Schermer and J. H. Cole, "Improved bend loss formula verified for optical fiber by simulation and experiment," *IEEE J. Quantum Electron.*, vol. 43, no. 10, pp. 899–909, Oct. 2007.

[21] A. Iadicicco, D. Paladino, M. Moccia, G. Quero, S. Campopiano, W. J. Bock, and A. Cusano, "Mode coupling and field distribution in sub-mm permanently bent single mode optical fibers," *Opt. Laser Technol.*, vol. 47, pp. 292–304, Apr. 2013.

[22] R. Morgan, J. S. Barton, P. G. Harper, and J. D. C. Jones, "Temperature dependence of bend loss in monomode optical fibers," *Electron. Lett.*, vol. 26, no. 13, pp. 937–939, Jun. 1990.

[23] F. M. Haran, J. S. Barton, S. R. Kidd, and J. D. C. Jones, "Optical fiber interferometric sensors using buffer guided light," *Meas. Sci. Technol.*, vol. 5, pp. 526–530, May 1994.

[24] G. Rajan, Y. Semenova, P. Wang, and G. Farrell, "Temperature-induced instabilities in macro-bend fiber based wavelength measurement systems," *J. Lightw. Technol.*, vol. 27, no. 10, pp. 1355–1361, May 2009.

[25] G. Rajan, Y. Semenova, and G. Farrell, "All-fiber temperature sensor based on macro-bend singlemode fiber loop," *Electron. Lett.*, vol. 44, no. 19, pp. 1123–1124, Sep. 2008.

[26] S. H. Nam and S. Z. Yin, "High-temperature sensing using whispering gallery mode resonance in bent optical fibers," *IEEE Photon. Technol. Lett.*, vol. 17, no. 11, pp. 2391–2393, Nov. 2005.

[27] G. L. Yin, S. Q. Lou, and H. Zou, "Refractive index sensor with asymmetrical fiber Mach-Zehnder interferometer based on concatenating single-mode abrupt taper and core-offset section," *Opt. Laser Technol.*, vol. 45, pp. 294–300, Feb. 2013.

[28] X. Shu, T. Allsop, B. Gwandu, L. Zhang, and I. Bennion, "Room- temperature operation of widely tunable loss filter," *Electron. Lett.*, vol. 37, no. 4, pp. 216–217, Feb. 2001.
[29] A. Priyadarshi, L. Shimin, S. G. Mhaisalkar, R. Rajoo, E. H. Wong, V. Kripesh, and E. B. Namdas, "Characterization of optical properties of acrylate based adhesives exposed to different temperature conditions," *J. Appl. Polym. Sci.*, vol. 98, pp. 950–956, Nov. 2005.

Jun He received the B.Eng. degree in electronic science and technology from Wuhan University, Wuhan, China, in 2006, and the Ph.D. degree in electrical engineering from the Institute of Semiconductors, Chinese Academy of Sciences, Beijing, China, in 2011.

From 2011 to 2013, he was with Huawei Technologies, Shenzhen, China, as a Research Engineer and worked on performance monitoring for agile optical networks. Since 2013, he has been with Shenzhen University, Shenzhen, China, as a Postdoctoral Research Fellow. His current research interests include optical fiber sensors, fiber Bragg gratings, and optical signal processing.He has authored or coauthored four patent applications and more than 30 journal and conference papers.

Changrui Liao received the B.S. degree in optical information science and technology and the M.S. degree in physical electronics from the Huazhong University of Science and Technology, Wuhan, China, in 2005 and 2007, respectively, and the Ph.D. degree in electrical engineering from the Hong Kong Polytechnic University, Hung Hom, Hong Kong, in 2012.

He is currently with Shenzhen University, Shenzhen, China, as an Assistant Professor. His current research interests include optical fiber sensors and femto second laser micro machining. He has authored or coauthored tenpatent applications and more than 60 journal and conference papers.

Kaiming Yang received the B.S. degree in optical information science and technology from East China Jiao Tong University, Nanchang, China, in 2012. He is currently working toward the Ph.D. degree in optical engineering in Shenzhen University, Shenzhen, China. His current research interests include optical fiber sensors and fiber Bragg gratings.

Shen Liu received the M.S. degree in electrical engineering from Chongqing University of Posts and Telecommunications, Chongqing, China, in 2012. He is currently working toward the Ph.D. degree in optical engineering in Shenzhen University, Shenzhen, China. His current research interests include optical fiber sensors and devices.

Guolu Yin received the B.S. and Ph.D. degrees in electronic science and technology from Beijing Jiao Tong University, Beijing, China, in 2008 and 2013, respectively. Since 2013, he has been with Shenzhen University, Shenzhen, as a Postdoctoral Research Fellow. His current research interests include optical fiber sensors and fiber gratings.

Bing Sun received the B.S. degree in optical information science and technology from Changchun University of Science and Technology, Changchun, China, in 2008, and Ph.D. degree in mechanical engineering from Jiangsu University, Zhenjiang, China, in 2013. Since 2013, he has been with Shenzhen University, Shenzhen, as a Postdoctoral Research Fellow. His current research interests include photonic crystal fiber devices.

Jiangtao Zhou is currently working towardthe M.S. degree in optical engineering in Shenzhen University, Shenzhen, China. His current research interests include optical fiber sensors and devices.

Jing Zhao is currently working toward the Ph.D. degree in optical engineering in Shenzhen University, Shenzhen, China. Her current research interests include optical fiber SPR sensors and biochemical sensors.

Yiping Wang (SM'11) received the B.Eng. degree in precision instrument engineering from the Xi'an Institute of Technology, Xi'an, China, in 1995, and the M.S. degree in precision instrument and mechanism and the Ph.D. degrees in optical engineering from Chongqing University, Chongqing, China, in 2000 and 2003, respectively.

He is currently a Distinguished Professor and a Pearl River Scholar in College of Optoelectronic Engineering, Shenzhen University, Shenzhen, China. From 2003 to 2005, he was with the Department of Electronics Engineering, Shanghai Jiao Tong University, Shanghai, China as a Postdoctoral Fellow and an Associate Professor. From 2005 to 2007, he was with the Department of Electrical Engineering, the Hong Kong Polytechnic University as a Postdoctoral Research Fellow. From 2007 to 2009, he was with the Institute of Photonic Technology, Jena, Germany, as a Humboldt Research Fellow. From 2009 to 2011, he was with the Optoelectronics Research Centre (ORC), University of Southampton, Southampton, U.K., as a Marie Curie Fellow. Since 2012, he has been with Shenzhen University, Shenzhen, China, as a Distinguished Professor and a Pearl River Scholar. His current research interests include optical fiber sensors, fiber gratings, and photonic crystal fibers. He has authored or coauthored one book, nine patent applications, and more than 150 journal and conference papers with a SCI citation of more than 1200 times. He is a Senior Member of the Optical Society of America and the Chinese Optical Society. He received the prestigious award of the National Excellent Doctoral Dissertation of China.